


**RESEARCH ARTICLE**

# Concurrent axon and myelin destruction differentiates X-linked adrenoleukodystrophy from multiple sclerosis

Caroline G. Bergner<sup>1,2</sup>  | Nafiye Genc<sup>1</sup> | Simon Hametner<sup>3</sup> | Jonas Franz<sup>1,4,5</sup> | Franziska van der Meer<sup>1†</sup> | Miso Mitkovski<sup>6</sup> | Martin S. Weber<sup>2</sup> | Gisela Stoltenburg-Didinger<sup>7</sup> | Jörn-Sven Kühl<sup>8</sup> | Wolfgang Köhler<sup>9</sup> | Wolfgang Brück<sup>1</sup> | Jutta Gärtner<sup>10</sup> | Christine Stadelmann<sup>1</sup>

<sup>1</sup>Institute of Neuropathology, University Medical Center Göttingen, Göttingen, Germany

<sup>2</sup>Department of Neurology, University Medical Center Göttingen, Göttingen, Germany

<sup>3</sup>Division of Neuropathology and Neurochemistry, Department of Neurology, Medical University Vienna, Vienna, Austria

<sup>4</sup>Max Planck Institute for Experimental Medicine, Göttingen, Germany

<sup>5</sup>Campus Institute for Dynamics of Biological Networks, University of Göttingen, Göttingen, Germany

<sup>6</sup>Light Microscopy Facility, Max-Planck Institute for Experimental Medicine, Göttingen, Germany

<sup>7</sup>Institute of Cell Biology and Neurobiology, Charité University Medicine, Berlin, Germany

<sup>8</sup>Department of Pediatric Oncology, Hematology, and Hemostaseology, University of Leipzig Medical Center, Leipzig, Germany

<sup>9</sup>Department of Neurology, University of Leipzig Medical Center, Leipzig, Germany

<sup>10</sup>Department of Pediatrics and Adolescent Medicine, University Medical Center Göttingen, Göttingen, Germany

**Correspondence**

Christine Stadelmann, Institute of Neuropathology, University Medical Center Göttingen, Robert-Koch-Straße 40, 37075, Göttingen, Germany.  
Email: cstadelmann@med.uni-goettingen.de

**Funding information**

Association Européenne contre les Leucodystrophies; Deutsche Forschungsgemeinschaft; Deutsche Multiple Sklerose Gesellschaft; Gemeinnützige Hertie-Stiftung; National Multiple Sclerosis Society

**Abstract**

Cerebral disease manifestation occurs in about two thirds of males with X-linked adrenoleukodystrophy (CALD) and is fatally progressive if left untreated. Early histopathologic studies categorized CALD as an inflammatory demyelinating disease, which led to repeated comparisons to multiple sclerosis (MS). The aim of this study was to revisit the relationship between axonal damage and myelin loss in CALD. We applied novel immunohistochemical tools to investigate axonal damage, myelin loss and myelin repair in autopsy brain tissue of eight CALD and 25 MS patients. We found extensive and severe acute axonal damage in CALD already in prelesional areas defined by microglia loss and relative myelin preservation. In contrast to MS, we did not observe selective phagocytosis of myelin, but a concomitant decay of the entire axon-myelin unit in all CALD lesion stages. Using a novel marker protein for actively remyelinating oligodendrocytes, breast carcinoma-amplified sequence (BCAS) 1, we show that repair pathways are activated in oligodendrocytes in CALD. Regenerating cells, however, were affected by the ongoing disease process. We provide evidence that—in contrast to MS—selective myelin phagocytosis is not characteristic of CALD.

<sup>†</sup>Deceased 9 November 2020

This is an open access article under the terms of the Creative Commons Attribution-NonCommercial-NoDerivs License, which permits use and distribution in any medium, provided the original work is properly cited, the use is non-commercial and no modifications or adaptations are made.

© 2021 The Authors. GLIA published by Wiley Periodicals LLC.

On the contrary, our data indicate that acute axonal injury and permanent axonal loss are thus far underestimated features of the disease that must come into focus in our search for biomarkers and novel therapeutic approaches.

#### KEYWORDS

axonal injury, demyelination, multiple sclerosis, remyelination, X-linked adrenoleukodystrophy

## 1 | INTRODUCTION

X-linked adrenoleukodystrophy (X-ALD), the most common peroxisomal hereditary leukodystrophy, is caused by a mutation in the *ABCD1* gene (Berger & Gärtner, 2006; Engelen, Kemp, & Poll-The, 2014; Mosser et al., 1993). It encodes the *ABCD1* transporter which shuttles activated, very long chain fatty acids (VLCFA) into the peroxisome where terminal degradation steps take place. Due to defects in this transport machinery, VLCFAs accumulate in all cells, tissues and body fluids of X-ALD patients (Kemp et al., 2001; Theda, Moser, Powers, & Moser, 1992). About two-thirds of male patients carrying the mutation develop CALD which, if left untreated, usually has a lethal course within months to a few years (de Beer, Engelen, & van Geel, 2014; Mahmood, Raymond, Dubey, Peters, & Moser, 2007; Raymond et al., 2019).

First seminal histological studies on CALD identified massive infiltration of lipid-laden macrophages and perivascular monocytes into the white matter in association with the destruction of myelin as outstanding and characteristic histopathologic features (Schaumburg, Powers, Raine, Suzuki, & Richardson, 1975). The inferred classification of CALD as an *inflammatory demyelinating* disease has repeatedly generated comparisons between CALD pathology and multiple sclerosis (MS; Berger, Forss-Petter, & Eichler, 2014; Moser, Naidu, Kumar, & Rosenbaum, 1987).

Although there has always been critical awareness of clinical and pathologic differences, a recent detailed comparison of the *inflammatory* component in the two diseases has helped elucidate these differences. We and others identified the loss of microglia cells in prelesional white matter areas (PL) as a unique and early feature in CALD lesion development (Bergner et al., 2019; Eichler et al., 2008). In addition, CNS-infiltrating peripheral monocytes in CALD showed a pro-inflammatory skewed expression profile compared to MS (Weber et al., 2014; Weinhofer et al., 2018). These findings could help to explain the differences in the clinical course between CALD and MS: While remitting inflammatory bouts are characteristic of the early disease phase in MS, inflammatory cell infiltration in CALD is in general not self-limiting and disease evolution fatally progressive, especially once a major disruption of the blood-brain-barrier has occurred (Liberato et al., 2019; Musolino et al., 2015). However, spontaneous arrest of the cerebral disease is found in approximately 12% of CALD patients (Mallack et al., 2020).

A similarly detailed comparison of *demyelination* and *axonal damage* in the two diseases is still lacking. In fact, while for MS there is abundant data on damage and repair of the axon-myelin unit, much less is known about de- and remyelination and concomitant axonal injury in CALD.

In the present work we strived to systematically assess demyelination and axonal changes along areas of lesion development in eight

autopsy cases of CALD. We observed that acute axonal injury occurs early on in lesion development, and to a striking extent. In contrast to MS, acute axonal damage in CALD was not contingent on inflammatory cell infiltration. Moreover, even in advanced lesion areas we did not find that myelin was primarily targeted for degradation, but instead observed a concurrent breakdown of the entire axon-myelin unit. Attempts at remyelination occurred in the CALD cases, but appeared to be hindered by ongoing tissue destruction as well as the lack of preserved axons that could serve as substrates for myelin repair.

## 2 | MATERIALS AND METHODS

### 2.1 | Human tissue

CALD lesion evolution was studied in formalin-fixed, paraffin-embedded (FFPE) autopsy brain tissue from eight patients obtained from the archives of the Institute of Neuropathology at the University Medical Center Göttingen, the Department of Neuropathology at the Charité Berlin, and from the Department of Neuropathology at the Medical University Vienna. The patient data are summarized in (Table 1). Patients with childhood, adolescent and adult disease variants were analyzed. We classified CALD lesion areas as proposed recently (Bergner et al., 2019), with some minor modifications. We distinguished *normal-appearing white matter* (NAWM) with regular microglia as determined by immunohistochemistry (IHC), *prelesional areas* (PL) with a reduction in microglia density and loss of homeostatic phenotype but largely unaltered myelin and oligodendrocytes, foam cell-rich, *actively resorptive areas* (AR) where major tissue phagocytosis occurred, and *gliotic areas* (GL) characterized by progressive astrocytic scarring.

Axon and myelin pathology in CALD was compared to lesions of 25 patients with chronic MS classified according to (Kuhlmann et al., 2017). Different MS lesion types were selected for specific comparisons with CALD lesion evolution in order to best match the degree of phagocyte infiltration and myelin degradation between the diseases: Findings in AR areas were contrasted with active and demyelinating or mixed active-inactive and demyelinating lesions (hereafter both designated active lesions; seven lesions in 6/25 patients). Here, dense infiltration of macrophages was found throughout the lesion area (active) or at the lesion border (mixed active/inactive), and ongoing myelin phagocytosis was indicated by myelin basic protein (MBP)- or Luxol-Fast-Blue (LFB)-positive myelin fragments in phagocytes. GL areas in CALD were contrasted with inactive lesions



TABLE 1 Clinical patient data

Case	Sex	Age (ys)	Disease duration (ys)	Disease course	Lesion areas/types
CALD1	M	9	1,25	Childhood	NAWM, PL, AR, GL
CALD2	M	16	6	Adolescent	GL
CALD3	M	46	n.a.	Adult	NAWM, PL, AR, GL
CALD4	M	55	n.a.	Adult	NAWM, PL, AR
CALD5	M	11	n.a.	Adolescent	NAWM, AR, GL
CALD6	M	9	n.a.	Childhood	AR, GL
CALD7	M	23	n.a.	Adult	NAWM, PL, AR
CALD8	M	14	n.a.	Adolescent	NAWM, PL
MS1	M	51	8	PPMS	Active and demyelinating
MS2	M	59	23	SPMS	Active and demyelinating, RM
MS3	M	59	26	SPMS	Active and demyelinating, inactive
MS4	M	28	3	PPMS	Mixed active-inactive and demyelinating
MS5	F	44	n.a.	n.a.	Mixed active-inactive and demyelinating
MS6	F	49	31	PPMS	Mixed active-inactive and demyelinating, inactive and postdemyelinating RM
MS7	n.a.	n.a.	21	SPMS	Inactive and postdemyelinating
MS8	F	34	15	RRMS	Inactive and postdemyelinating
MS9	F	44	15	PPMS	Inactive and postdemyelinating
MS10	F	52	19	Chronic MS	Inactive and postdemyelinating
MS11	F	57	32	SPMS	Inactive and postdemyelinating
MS12	M	65	n.a.	n.a.	Inactive and postdemyelinating
MS13	M	63	n.a.	n.a.	Inactive and postdemyelinating, RM
MS14	M	49	n.a.	n.a.	Inactive and postdemyelinating
MS15	F	59	16	Chronic MS	inactive and postdemyelinating
MS16	M	57	5	Chronic MS	Inactive and postdemyelinating
MS17	F	47	24	SPMS	Inactive and postdemyelinating
MS18	F	40	n.a.	n.a.	RM
MS19	M	41	n.a.	n.a.	RM
MS20	M	61	18	SPMS	RM
MS21	M	69	7	SPMS	RM
MS22	F	58	n.a.	SPMS	RM
MS23	M	55	>15	Chronic MS	RM
MS24	M	54	11	SPMS	RM
MS25	M	34	3	Chronic MS	RM
C1	M	8		Control	NWM
C2	F	11		Control	NWM
C3	M	11		Control	NWM
C4	F	19		Control	NWM
C5	M	19		Control	NWM
C6	M	26		Control	NWM
C7	F	38		Control	NWM
C8	F	38		Control	NWM
C9	F	39		Control	NWM
C10	F	40		Control	NWM
C11	M	46		Control	NWM
C12	F	57		Control	NWM

TABLE 1 (Continued)

Case	Sex	Age (ys)	Disease duration (ys)	Disease course	Lesion areas/types
C13	M	58		Control	NWM
C14	M	60		Control	NWM
C15	M	62		Control	NWM
C16	M	65		Control	NWM

Abbreviations: AR, actively resorptive area; C, control individuals; CALD, cerebral X-linked adrenoleukodystrophy; F, female; GL, gliotic area; M, male; MS, multiple sclerosis; n.a., clinical data not available; NAWM, Normal appearing white matter; NWM, normal white matter; PL, prelesion; PPMS, primary progressive MS; RM, remyelinated lesion; RRMS, relapsing remitting MS; SPMS, secondary progressive MS; ys, years.

(13 lesions from 13/25 patients) where activated microglia/macrophages were largely absent. Further clinical and histopathologic characteristics of the patients studied are provided in (Table 1). Furthermore, we classified the lesions according to the extent of remyelination (Patrikios et al., 2006): Lesions with circumscribed pale LFB staining sharply demarcated from the surrounding white matter were classified as remyelinated (14 shadow plaques/shadow plaque areas in 12/25 MS patients). Periplaque areas in MS, used for quantification of amyloid precursor protein (APP), were defined within a distance of 0.25 mm to the border of active lesions (one ocular grid at  $\times 400$  magnification). Tissue from 16 individuals without confounding CNS pathology, aged between 8 and 65 years, served as a control (Table 1). The study was approved by the ethical review committee of the University Medical Center Göttingen.

## 2.2 | Histology and immunohistochemistry

Sections were stained with hematoxylin and eosin (HE), Luxol Fast Blue/periodic-acid Schiff (LFB/PAS) and Bielschowsky silver-impregnated according to standard procedures to assess cellularity, myelin, and axonal density. IHC was performed with primary and secondary antibodies listed in (Table S1). To achieve a high sensitivity for remaining axon fragments, we employed a cocktail of neurofilament antibodies containing neurofilament (NF), NF200, SMI31, SMI32, SMI35, and SMI312, hereafter referred to as pan-neurofilament (pan-NF) IHC. Tissue antigens were visualized by biotinylated secondary antibodies, peroxidase-conjugated avidin, and diaminobenzidine (DAB, Sigma-Aldrich). Double-labeling IHC was performed combining DAB with alkaline phosphatase-conjugated antibodies and Fast Blue (Sigma-Aldrich).

## 2.3 | Morphometric analysis

Lesion areas in CALD were classified based on the characteristics described above, and quantification of cell and axon density was performed as described previously (Bergner et al., 2019; Brück et al., 1997). Results are given as cells/mm<sup>2</sup> or relative axon density compared to age- and region-matched controls. To determine the myelination status of damaged axons, APP or pan-NF and MBP-double-labeled sections were analyzed. To search for signs of axon

phagocytosis, NF200 and CD68 equivalent Ki-M1P (Radzun et al., 1991) double-labeled sections were scanned for intracytoplasmic axon fragments. All breast carcinoma-amplified sequence 1 (BCAS1)- as well as all fluorescently labeled sections were digitalized using the virtual slide microscope VS 120 and analyzed using the VS-ASW software (at  $\times 200$  or  $\times 400$  magnification, Olympus, Germany) or the Leica SP2 laser scanning confocal microscope ( $\times 400$  magnification, Leica Microsystems, Germany) with subsequent analysis in Fiji (v.1.52v NIH, USA).

## 2.4 | Statistical analysis

All statistics were calculated using the GraphPad Prism 6 software (GraphPad Software, La Jolla, CA) or open source python packages (stats from library SciPy 1.0, statsmodel). Data are represented as mean  $\pm$  standard error of the mean (SEM) computed from quantifications of randomly selected parts of the lesion areas within the indicated patient or lesion or, in the case of BCAS1 IHC, counted within an entire lesion area of a specific tissue block. For CALD lesion areas and in controls, data are represented as mean  $\pm$  SEM of quantifications over all available tissue blocks of one patient, containing the specific area. Only for the computation of the regression curve of macrophage density versus APP, average cell numbers obtained from different blocks were analyzed separately. In MS, data are represented as mean  $\pm$  SEM computed separately from quantification of each specific lesion. Usually 10, but at least five randomly sampled parts of a lesion area were quantified for the computation of average counts.

For comparisons of different lesion areas within a disease, one-way ANOVA and, for analysis of the effects of disease (MS compared to CALD) in different lesion areas, two-way ANOVA ("density  $\sim$  C(disease) + C(area) + C(disease):C(area)", ANOVA type III) were performed as indicated in the figure legends. Residuals of the ANOVA were tested for normality in QQ Plot (Figure 1b and 5n: Logarithm of density [shifted density in Figure 1b: +0.1, to avoid zero density]). A significant main effect of disease (df = 1,  $F = 9.97$ ,  $p = .0031 < .01$ ), lesion area (df = 3,  $F = 32.55$ ,  $p < .0001$ ) and significant interaction term of disease and area (df = 3,  $F = 7.21$ ,  $p = .0022 < .001$ ) were found for relative axonal densities (Figure 1a), and a significant main effect of disease (df = 1,  $F = 6.87$ ,  $p = .0129 < .05$ ), lesion area (df = 3,  $F = 46.06$ ,  $p < .0001$ ) and significant interaction term of disease and area (df = 3,  $F = 8.90$ ,  $p = .00077 < .001$ ) were found for

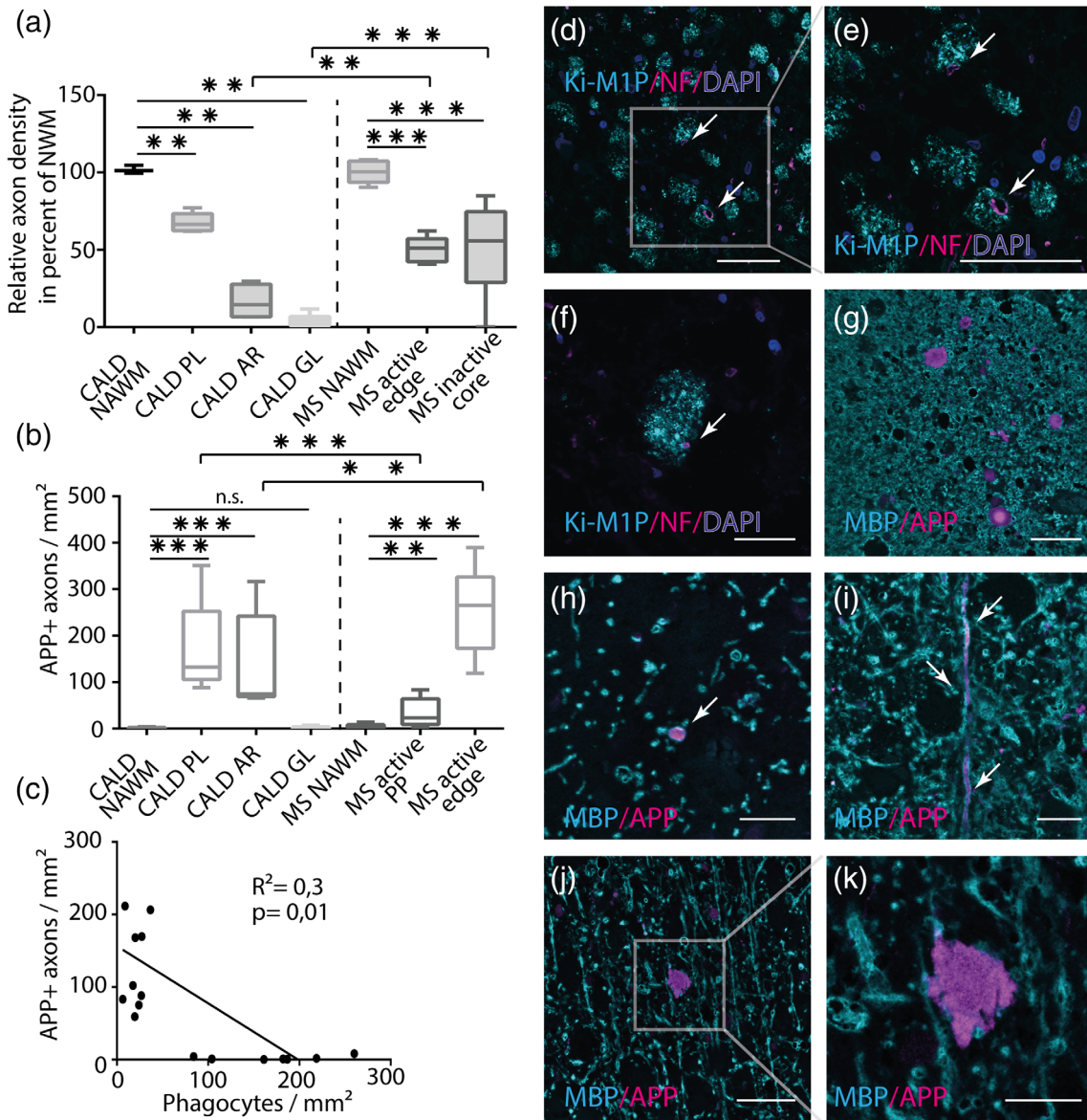


**FIGURE 1** Axonal loss and acute axonal damage in CALD lesions. (a) Relative axon densities in lesion areas of CALD and MS. Densities were determined in Bielschowsky silver impregnation and normalized to age- and region-matched controls. (b) APP+ axons in the different stages of lesion development in CALD and MS. (c) APP+ axonal profiles are inversely correlated to macrophage density in PL and NAWM areas of CALD ( $p = .014$ ,  $R$  square = 0.32). CALD NAWM, CALD normal-appearing white matter; CALD PL, CALD prelesion; CALD AR, CALD actively resorptive area; CALD GL, CALD gliotic area; MS NAWM, NAWM in MS; MS active edge, foam cell-rich lesion edge with evidence of demyelination in MS; MS active PP, periplaque area of active MS lesion (defined as the area within 0.25 mm distance from lesion edge); MS inactive core, gliotic lesion center of inactive MS lesions; n.s., not significant. (d–f) Double immunohistochemistry (IHC) of neurofilaments (NF200: magenta) and macrophages (Ki-M1P: cyan, DAPI: blue) reveals intracellular neurofilament inclusions (arrows) as signs of ongoing axon phagocytosis. (g) APP+ axons in PL areas are tightly surrounded by myelinated fibers. Here, an unambiguous evaluation whether a specific damaged axon is myelinated or embedded in surrounding myelin often is not possible. (h, i) In AR areas, APP+ axons are rarely covered by myelin (arrows). (j, k) APP+ axonal spheroids often show an irregular shape, potentially indicating membrane disruption, and closely contact or even surround neighboring structures. (g–k: APP: magenta, MBP: cyan). (a, b) Two-way ANOVA with Mann–Whitney tests for posthoc multiple comparisons. \* $p < .05$ ; \*\* $p < .01$ ; \*\*\* $p < .001$ . Scale bar: d, e, g, i, j: 50  $\mu$ m; f, h, k: 20  $\mu$ m

comparisons of APP+ axon densities (Figure 1b). One-way ANOVA revealed a significant change of BCAS1+ cell density for different areas ( $df = 3.22$ ,  $F = 7.354$ ,  $p = .001368 < .01$ , Figure 5n). Individual distributions within the ANOVA were tested for normality by Shapiro Wilks test ( $\alpha = 0.05$ , Figure 5n: normality was confirmed only for

logarithm of distributions). For non-parametric data, Mann–Whitney tests were used as posthoc multiple comparisons (Figure 1a,b) that underwent Holm–Sidak correction ( $\alpha_{\text{Sidak}} = 1 - [1 - \alpha]^{1/m}$ ,  $m$ th sorted comparison of all comparisons  $k = 11$ ). For parametric data, multiple  $t$ -tests with Bonferroni correction were applied

( $\alpha_{\text{Bonferroni}} = \alpha/k$ ,  $k$  = number of comparisons, Figure 5n). Levels of significance for multiple comparisons are reported in the figures/figure legends. To compare differences in myelination between two specific lesion areas in CALD and MS, Mann–Whitney test was applied (non-parametric data, Figure 4a). Significant deviations in BCAS1+ cell densities from control tissue in individual lesion areas and patients were assumed if values exceeded the threshold density of 1.327 cells/mm<sup>2</sup> (Figure 5o). Threshold was defined as upper limit of 99.9% confidence interval ( $\alpha = 0.001$ ), computed by back transformation from a normal distribution fitted to the logarithm of BCAS1+ cell densities in control tissue.

### 3 | RESULTS

#### 3.1 | Substantial axon loss in CALD lesions

First, we determined the extent of axon loss along the course of lesion development in CALD, relying on our previously established classification of lesion areas (Bergner et al., 2019). Quantification of axon density in Bielschowsky silver impregnated sections revealed a significant decrease in axon density already in prelesional areas (PL) compared to normal-appearing white matter (NAWM) ( $64.3 \pm 1.0\%$  of axon density in age-matched control tissue in PL areas vs.  $101.3 \pm 1.1\%$  in NAWM). Within actively resorptive (AR) and gliotic (GL) areas we observed a severe reduction, up to an almost complete loss of axons from GL lesion cores (early AR areas:  $16.3 \pm 5.7\%$  of control white matter axon density; GL areas:  $3.3 \pm 2.1\%$ ; Figure 1a). We directly compared this to axon loss in MS lesions. Axon density was significantly higher at the foam cell-rich edge of active MS lesions compared to AR areas in CALD. Likewise, axon density in the center of chronic inactive lesions significantly exceeded that in GL areas in CALD ( $50.0 \pm 3.7\%$  of axon density in age-matched control white matter at the edge of active MS lesions;  $52.9 \pm 8.0\%$  in inactive lesion cores; Figure 1a). To determine whether axon loss in CALD was accompanied by axon phagocytosis, we searched for axon fragments in macrophages on sections double-labeled for phagocytes (Ki-M1P/CD68) and neurofilament (NF 200). In addition, we screened the respective AR regions for the presence of BCAS1+ inclusions in phagocytes that indicate ongoing myelin degradation. We observed rare intracytoplasmic neurofilament inclusions in most of the early AR areas in CALD that displayed signs of ongoing myelin digestion, though less cells showed NF+ compared to BCAS1+ inclusions ( $n = 4$  cases with NF+ fragments out of five cases with BCAS1+ inclusions, Figure 1d–f).

#### 3.2 | Massive acute axonal damage is occurring already in prelesional areas of CALD

Next, we set out to assess localization and extent of acute axonal damage in CALD. Amyloid precursor protein (APP) is a cargo of fast axonal transport and accumulates in axons when this transport is disrupted (Koo et al., 1990), thus representing a surrogate of acute axonal damage. Quantifying the density of APP-positive axonal profiles along the different areas of lesion development in CALD, we observed a strong increase

in the density of APP+ damaged axons in PL areas ( $167.2 \pm 40.4$  axons/mm<sup>2</sup> in PL compared to  $2.2 \pm 1.1$  in NAWM; Figure 1b). PL areas were characterized by a severe reduction in phagocytic cells ( $27.0 \pm 5.0$  Ki-M1P+ cells/mm<sup>2</sup> in PL areas vs.  $142.1 \pm 21.2$  Ki-M1P+ cells/mm<sup>2</sup> in NAWM) and an absence of TMEM119+ and P2Y12+ homeostatic microglia ( $135.3 \pm 25.4$  P2Y12+ cells/mm<sup>2</sup> in NAWM vs.  $2.8 \pm 1.5$  P2Y12+ cells/mm<sup>2</sup> in PL), while myelin was not relevantly diminished (Figure 2a,b). Correspondingly, the density of APP+ axons was inversely correlated to Ki-M1P+ phagocytes when assessing PL and NAWM regions in CALD ( $p = .014$ , R square = 0.32; Figure 1c). In contrast, in MS the density of APP-accumulating axons was shown to correlate positively with macrophage infiltration (Bitsch, Schuchardt, Bunkowski, Kuhlmann, & Brück, 2000). Accordingly, while APP+ axon density was comparatively low in the periplaque area in MS ( $32.0 \pm 11.5$  APP+ axons/mm<sup>2</sup>), we found high densities of APP+ axons at the edge of active lesions intensely populated by activated microglia/macrophages. Here, APP+ axon density exceeded that found in AR areas of CALD ( $254.0 \pm 34.6$  APP+ axons/mm<sup>2</sup> at the lesion edge, Figure 1b, 2d–f). However, as demonstrated above, axon loss was more severe in foam cell-rich, resorptive lesion stages of CALD than at the foam cell-rich edge of active MS lesions. Therefore, even though the absolute numbers of APP+ axons were higher at the active lesion edge in MS (Figure 1b), the proportion of acutely damaged fibers among the few remaining axons might be even higher in CALD than in MS.

#### 3.3 | APP accumulation is observed in myelinated as well as non-myelinated axons

To investigate whether disturbance of axonal transport occurred more frequently in demyelinated axons, we double-labeled tissue for APP and MBP, thereby visualizing the myelination status of damaged axons. In PL areas of CALD, most APP+ axons were in immediate contact with myelin which, however, was densely packed, making it often hard to judge unambiguously whether the APP+ axon itself was covered by myelin or just tightly surrounded by other myelinated axons (Figure 1g). Nevertheless, we found clearly myelinated APP+ axons in later stage lesion areas, when axon density was substantially decreased, in all examined cases ( $n = 5$ ; Figure 1h,i). The vast majority of APP+ axonal profiles in these regions, however, was not covered by myelin. In general, APP+ axonal segments in CALD were longer and spheroids were larger compared to MS (Trapp et al., 1998). Interestingly, in AR areas of CALD, spheroids displayed very irregular shapes, seemingly lacking a surrounding membrane and in part flowing in between and around neighboring myelin tracts (Figure 1j,k).

#### 3.4 | No apparent selective demyelination in CALD lesions

So far, our results demonstrated severe damage and permanent loss of axonal structures in CALD. Such axon loss is expected to be accompanied by the decay of the covering myelin sheaths. We then proceeded to determine whether in addition to such secondary myelin

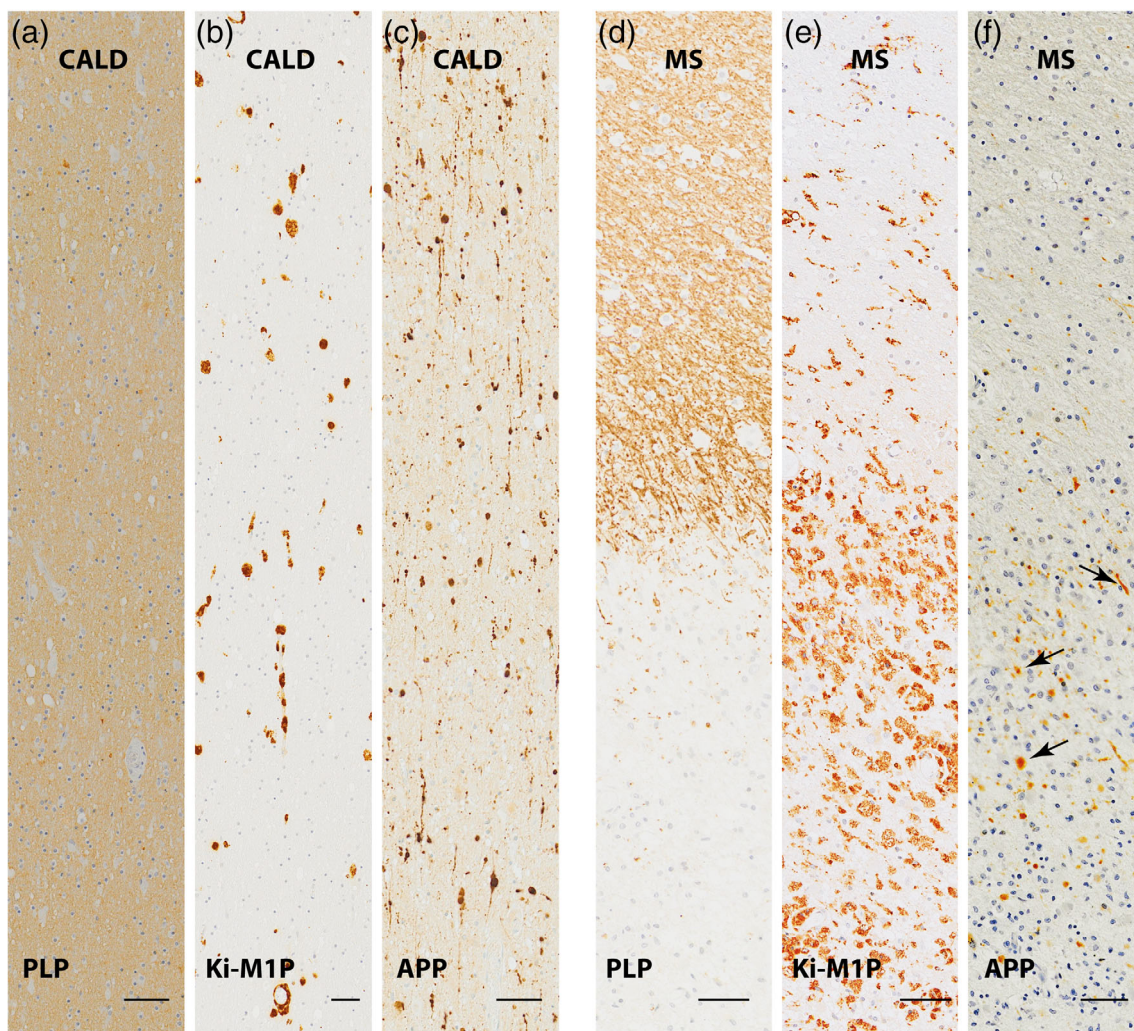


**FIGURE 2** Acute axonal damage in prelesional areas occurs independently of myelin loss and inflammatory cell infiltration. Serial sections of a prelesional area in CALD stained for (a) proteolipid protein (PLP), (b) CD68/Ki-M1P demonstrating severely reduced and mostly perivascular phagocytes and (c) amyloid precursor protein (APP) as marker of acute axonal damage. For comparison, the same immunohistochemical stainings are shown at the lesion edge of an active MS lesion (d–f). Note that the regions of highest APP density in MS (arrows on exemplary axons) correspond to areas of elevated phagocyte density, while in CALD, axons accumulate APP in extended regions with concomitant phagocyte loss and myelin that appears largely intact by IHC for myelin proteins. Scale bar: a–f: 50  $\mu$ m

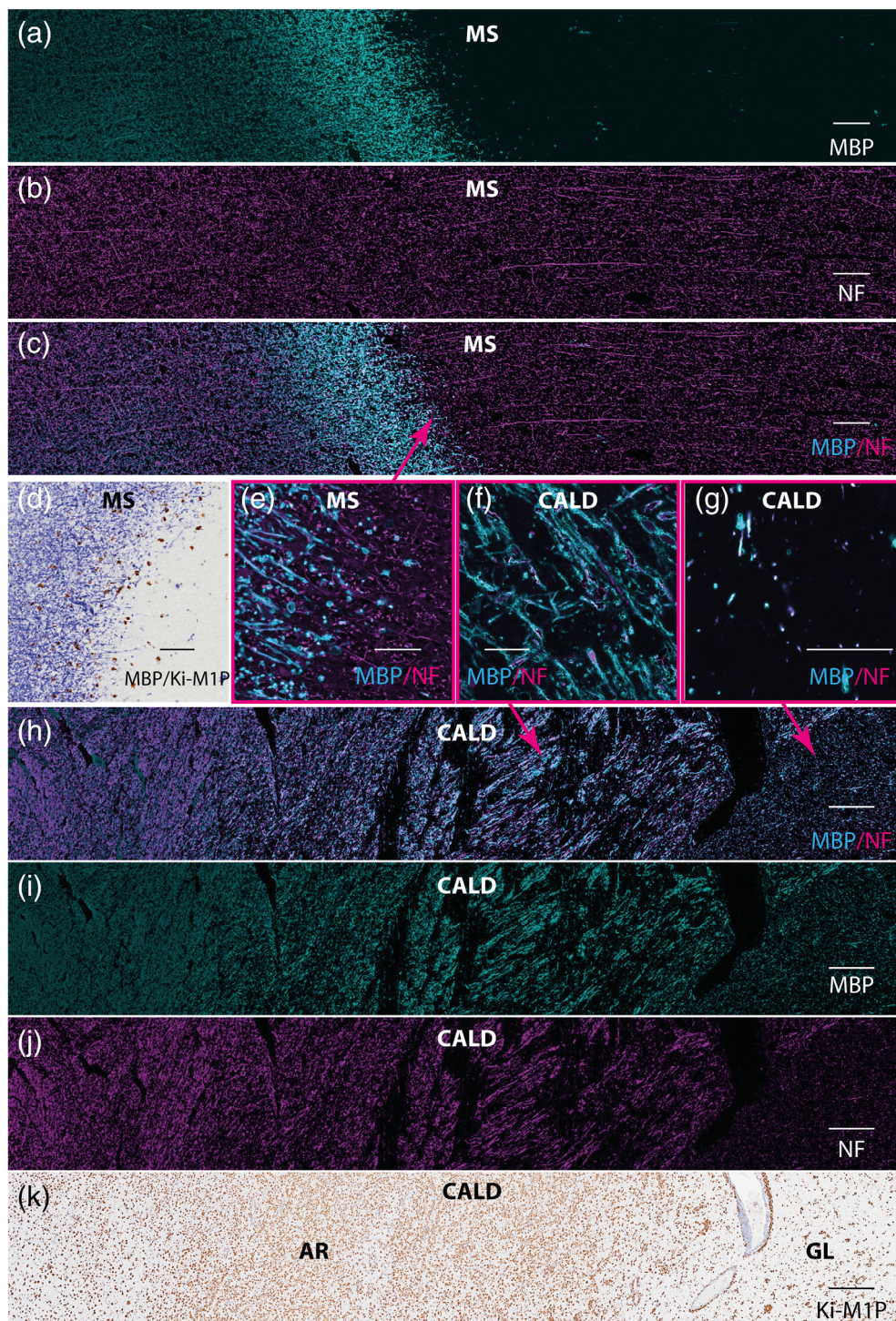
decay there was evidence for primary and selective phagocytic targeting of myelin in CALD. Selective demyelination as observed in MS lesions is characterized by the stripping of myelin sheaths from preserved axons. In the cases examined here, and as is characteristic for MS, this process resulted in sharply demarcated lesion edges in non-remyelinated inactive lesions. The transition from the periplaque white matter to complete loss of myelin was abrupt, as visualized by co-staining of myelin (MBP) and neurofilaments (pan-NF; Figure 3a–e). The border of active MS plaques was populated by foamy macrophages displaying signs of ongoing myelin degradation, as evidenced by the presence of intracellular myelin inclusions. Despite the ongoing tissue infiltration, the transition from myelinated to completely denuded axons was also spatially restricted and well demarcated (Figure 4b). In contrast, myelin reduction in early stage AR areas of CALD was far less demarcated and extended gradually over much longer distances (Figure 3f–k). Myelin in AR areas of CALD

often appeared morphologically altered, distended, vacuolized and partly detached from the axon (Figure 4c–e). Nevertheless, when quantifying the percentage of residual myelinated axons in MBP and pan-NF co-staining, we found the majority of axons were still surrounded by a covering myelin sheath, not only in AR but even in GL areas of CALD ( $69.0 \pm 8.2\%$  of remaining axons in AR areas and  $63.5 \pm 6.3\%$  in gliotic areas, Figure 3f, g; Figure 4a,c–e). In contrast, in active MS lesions the vast majority of axons behind the leading front of myelin phagocytosing foam cells were demyelinated ( $0.016 \pm 0.014\%$  of axons covered by myelin, Figure 4a,b).

### 3.5 | No evidence of shadow plaque areas in CALD

Remyelinated areas in MS were sharply demarcated from the surrounding normal-appearing tissue by pallor in LFB and myelin

**FIGURE 3** Selective demyelination as seen in MS is not found in CALD. (a–c) Fluorescently labeled section illustrating the extent of demyelination in a chronic demyelinated MS lesion. Myelin is completely absent from the lesion center (a, right hand side, MBP), while axonal structures prevail (b, pan-NF, c, merge). The lesion is classified as inactive due to the lack of accumulations of macrophages/activated microglia at the lesion border (d, blue: MBP, brown: Ki-M1P). Higher magnification of demyelination at the lesion border is shown in (e). For comparison, actively resorptive (AR, left hand side and center) and early gliotic (GL, right hand side) areas in a CALD lesion are presented with the same stainings (h: merge, i: MBP, j: pan-NF). Higher magnifications of (f) AR and (g) GL areas demonstrate that most of the remaining axons' surface is covered by myelin and that a joint decay of the entire axon-myelin unit occurs. On a serial section immuno-stained with Ki-M1P, macrophage accumulation indicates the extension of lesion areas (k). (a–c, e–j): pan NF: magenta, MBP: cyan). Scale bar: a–d: 100  $\mu$ m; e–g: 50  $\mu$ m; h–k: 500  $\mu$ m



protein staining (Figure 4f,g) associated with a thinned density of axonal fibers and myelin sheaths that appeared intact by light microscopy (Figure 4j,k). In contrast, in PL areas of CALD we found a *gradual* reduction in LFB staining (Figure 4h,i) not sharply delineated from the NAWM. The density of myelin did not appear reduced by myelin protein staining, but edematous alterations of myelin and axonal swellings prevailed (Bergner et al., 2019; Figure 2a and 4l).

To test at a cellular level whether ongoing attempts at remyelination existed in different lesion areas of CALD, we utilized a

recently characterized marker protein that identifies premyelinating and actively myelinating oligodendrocytes, breast carcinoma-amplified sequence 1 (BCAS1, Fard et al., 2017). Densities of myelinating oligodendrocytes with strong cytoplasmic and cell process expression of BCAS1 (Figure 5a,b) were elevated in shadow plaque areas with ongoing remyelination in MS (Figure 5c), as shown previously (Fard et al., 2017). In contrast, in completely remyelinated shadow plaques as well as in the white matter of adult controls cellular BCAS1 expression was low (Figure 5d,e). We did not find a significant increase in BCAS1+



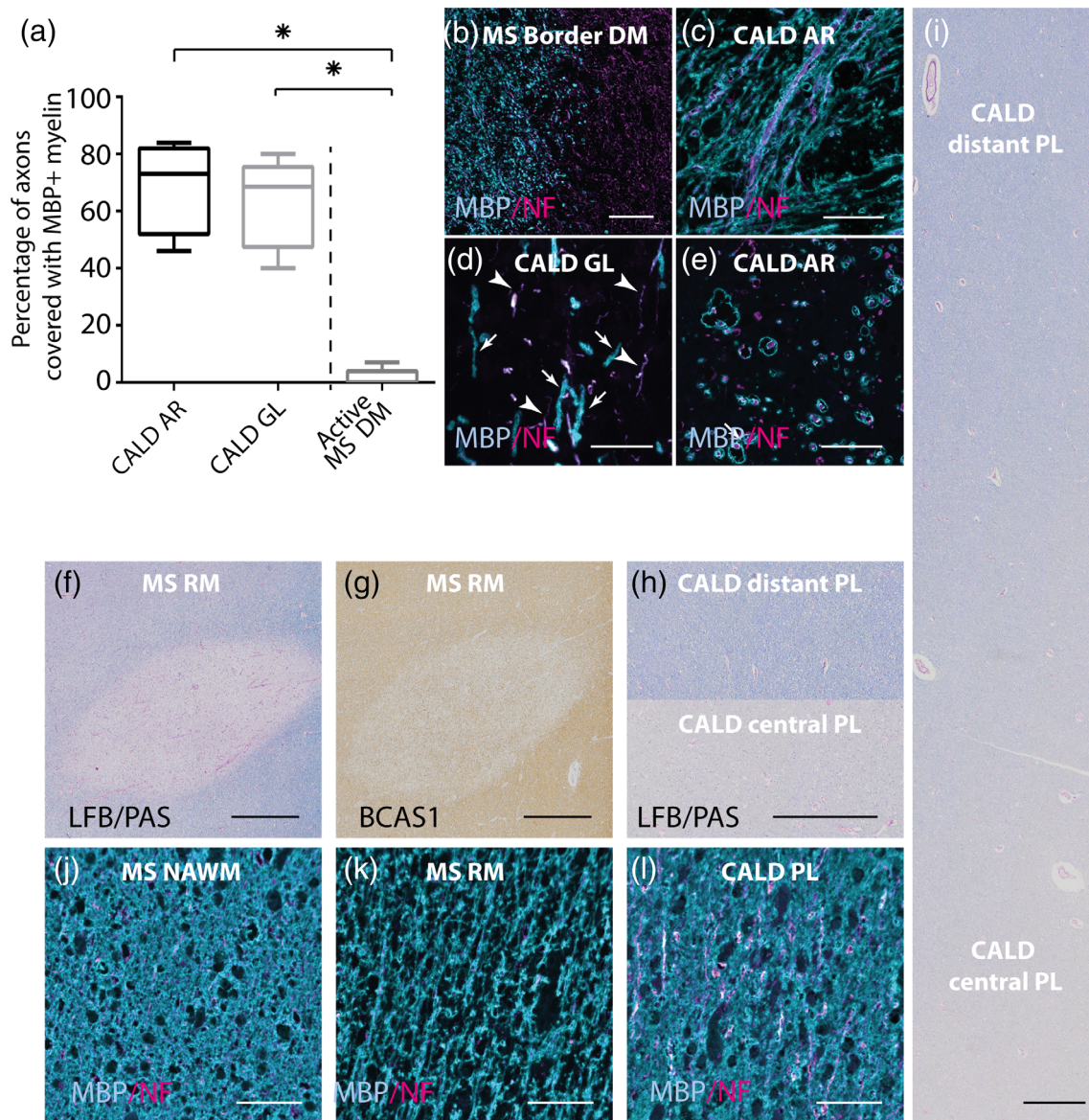


**FIGURE 4** No generic signs of successful remyelination in CALD. (a) Quantification of remaining axons covered by myelin in AR and GL areas in CALD, and directly behind the leading front of phagocytes at the edge of active MS lesions, in percent. The large majority of axons are denuded at the edge of active MS lesions as demonstrated by MBP and pan-NF double-IHC (b, MS4). Myelin covers most of the axons in AR (c, CALD 1) as well as GL (d, CALD 2) areas. Note that myelin in these regions often displays an altered morphology as visible also on a transversal section of an advanced AR area in (e, CALD 5). Shadow plaques in MS are delineated from the surrounding white matter by sharply demarcated pale LFB/PAS (f) and myelin protein (g, MS18) staining. In PL regions in CALD LFB pallor can be striking as demonstrated by a juxtaposition of PL areas distant and adjacent to the resorptive lesion part (h). However, in contrast to shadow plaques, myelin pallor increases gradually and is not sharply demarcated from the surrounding tissue (i, CALD4). Compared to adjacent NAWM (j) the density of myelin and axons is reduced in shadow plaque areas (k, MS18). In PL areas of CALD, in contrast, myelin density is not relevantly decreased according to immunohistochemistry, but axons often appear swollen (l, CALD1; b–e, j–l: pan NF: magenta, MBP: cyan). CALD AR: CALD actively resorptive area; CALD GL: CALD gliotic area; active MS DM: demyelinated area of active MS plaques directly behind the leading front of phagocytes at the lesion edge. (a) Mann-Whitney test. \* $p < .05$ . Scale bar: b: 100  $\mu\text{m}$ ; c–e, j–l: 50  $\mu\text{m}$ ; f–i: 500  $\mu\text{m}$

cell densities in the NAWM or in PL areas of CALD compared to age-matched controls ( $0.4 \pm 0.2$  and  $0.4 \pm 0.3$  BCAS1+ cells/ $\text{mm}^2$  in NAWM and PL; Figure 5n). In AR areas, process-bearing BCAS1+ cells frequently displayed an altered, distorted shape. In regions with high densities of phagocytes, these cells were often smudgy in appearance and processes were retracted and condensed around the cytoplasm (Figure 5f,g,h right hand side). Similar dysmorphic BCAS1+ cells were

not observed in any of the active MS lesions studied. Also, BCAS1 immunoreactivity was accentuated in the cytoplasm but not in the processes of a subset of presumably mature oligodendrocytes that assumed a ballooned shape in progressed AR areas (Figure 5i).

However, apart from these damaged oligodendrocytes, we were able to identify regenerating, process-bearing BCAS1+ cells in two out of six CALD cases harboring subcortical early stage AR areas with





minor inflammatory tissue infiltration (Figure 5h left hand side, j, k). There, the density of BCAS1+ cells was significantly higher than in control white matter (Figure 5n). Based on our previous findings (Fard et al., 2017), we compared these results to a cohort of remyelinated MS lesions (14 shadow plaques/shadow plaque areas from 12 patients). Among these we identified three lesions with ongoing remyelination, in which BCAS1+ cell densities were significantly elevated compared to control white matter (>99.9% confidence interval Figure 5o). Densities of BCAS+ regenerating cells in the two CALD cases were comparable to those in shadow plaques with ongoing remyelination in MS (Figure 5o).

In GL areas of CALD, we found few remaining oligodendrocytes in the tissue. These cells expressed BCAS1 in the cytosol, were mostly spheric and equipped with few or no processes (Figure 5l). Occasionally cells with the typical shape of remyelinating oligodendrocytes were observed (Figure 5m). In comparison, BCAS1+ cells were completely absent from lesion centers of chronic inactive MS lesions ( $2.1 \pm 0.7$  BCAS1+ branched and unbranched cells in GL areas in CALD vs.  $0.01 \pm 0.01$  BCAS1+ cells in MS lesion centers [seven chronic inactive lesions in five patients],  $p = .001$ , Mann-Whitney test).

## 4 | DISCUSSION

We observed early and extensive axonal damage, later-stage subtotal axon loss and no evidence for selective myelin phagocytosis in brain lesions of patients with cerebral X-ALD. Thus, our data indicate that axonal and myelin pathology go hand in hand in CALD lesion evolution. We did not find clear evidence of sustained remyelination, and the observation of substantial axon damage suggests that isolated attempts at stimulating myelin repair will not likely lead to clinical stabilization or improvement. Our direct comparison of axonal and myelin pathology in CALD with the prototypic demyelinating disease MS casts doubt on the classification of CALD as a primary demyelinating disease. In line, recent findings demonstrated an early impact upon glial cells, in particular microglia and astrocytes, in pre-phagocytic lesion areas (Bergner et al., 2019; Görtz et al., 2018).

While in MS oligodendrocytes and myelin are considered the prime targets of the disease process, axonal injury and neuro-axonal degeneration are regarded to be the major structural correlates of permanent disability (Bjartmar, Kidd, Mörk, Rudick, & Trapp, 2000; Charcot, 1868; Trapp et al., 2018). In MS, acute axonal damage correlates with the density of macrophages/activated microglia and lymphocytes in actively demyelinating lesions (Bitsch et al., 2000; Ferguson, Matyszak, Esiri, & Perry, 1997; Frischer et al., 2009; Kuhlmann, Lingfeld, Bitsch, Schuchardt, & Brück, 2002) and is for the most part attributable to the highly toxic inflammatory lesion microenvironment. Neurotoxic cytokines, chemokines and in particular reactive oxygen and nitrogen species impair mitochondrial respiration and axonal energy supply (Mahad, Trapp, & Lassmann, 2015), leading to intra-axonal calcium overload, protease activation and cytoskeletal breakdown (Siffrin et al., 2010; Stys, 2005; Yang et al., 2013). We

demonstrate here that acute axonal damage in CALD occurs already in PL areas, and to a striking extent. Interestingly, this is in line with evidence from magnetic resonance spectroscopy (MRS) studies which demonstrate low total N-acetylaspartate (tNAA), a surrogate marker of axonal damage, in areas beyond the destructive lesion (Eichler, Barker et al., 2002; Eichler, Itoh et al., 2002). In contrast to MS, the density of activated microglia/macrophages is low in PL regions in CALD and even reduced compared to the NAWM (Figure 6a,c). Therefore, while the inflammatory environment in CALD lesions may contribute to axonal injury during further lesion development, inflammatory bystander damage is unlikely to underlie the massive axonal damage observed in early pre-phagocytic lesion areas of CALD.

Mouse models of X-ALD do not develop cerebral disease, but show an age-dependent dying back degeneration of long spinal axon tracts, reminiscent of the human AMN phenotype (Pujol et al., 2002; Pujol et al., 2004). It is an open question whether the same mechanisms that confer length-dependent vulnerability to axons in AMN could gain relevance focally also in prelesional areas of CALD white matter. In fact, evidence has been provided that dying back axonopathy, also in other conditions, is a multifocal process that probably just prevails mostly in distal axon parts of long tracts, due to highest demands on intact transport machineries in these remote cellular compartments (Coleman, 2005; Spencer & Schaumburg, 1977a, 1977b). The mechanisms by which axonal injury occurs in AMN are, however, not fully understood. It has been hypothesized that incorporation of VLCFA into the mitochondrial membrane fuels the generation of reactive oxygen species which might instigate axonal damage via the above pictured pathogenic cascades (Fourcade, Ferrer, & Pujol, 2015). However, ABCD1 deficiency is largely compensated for by its homologue transporters ABCD2 and ABCD3. Expression of ABCD1 is low in neurons compared to its homologues, while it is highly abundant in glia cells (Fouquet et al., 1997; Höftberger et al., 2007). Accordingly, it has been argued that axonal damage in X-ALD most likely does not result from a cell autonomous pathogenic process alone, but rather develops secondary to glial cell damage (Berger et al., 2014; Gong et al., 2017).

In this regard, it has to be stressed that the most pronounced alterations in prelesional areas are found in myeloid cells. They are severely diminished in PL areas, lose homeostatic marker proteins such as TMEM119, and the few remaining cells show activated morphologies and increased rates of cell death (Bergner et al., 2019). In fact, loss of myeloid cell function may represent an important checkpoint in lesion formation, increase the metabolic burden on the tissue, and contribute to triggering the demise of axons and other glial cell types within PL areas (Figure 6). In this respect, parallels can be drawn to another rare white matter disease, adult onset leukodystrophy with axonal spheroids and pigmented glia (ALSP), a hereditary leukodystrophy associated with hetero- and homozygous mutations in the CSF1 receptor (Konno, Kasanuki, Ikeuchi, Dickson, & Wszolek, 2018). Histopathologically, this disease is characterized by a prominent reduction in microglia cells in association with extensive axonal damage reflected by high numbers of APP-positive axonal spheroids as a characteristic hallmark (Oosterhof et al., 2019; Oyanagi et al., 2017). In the

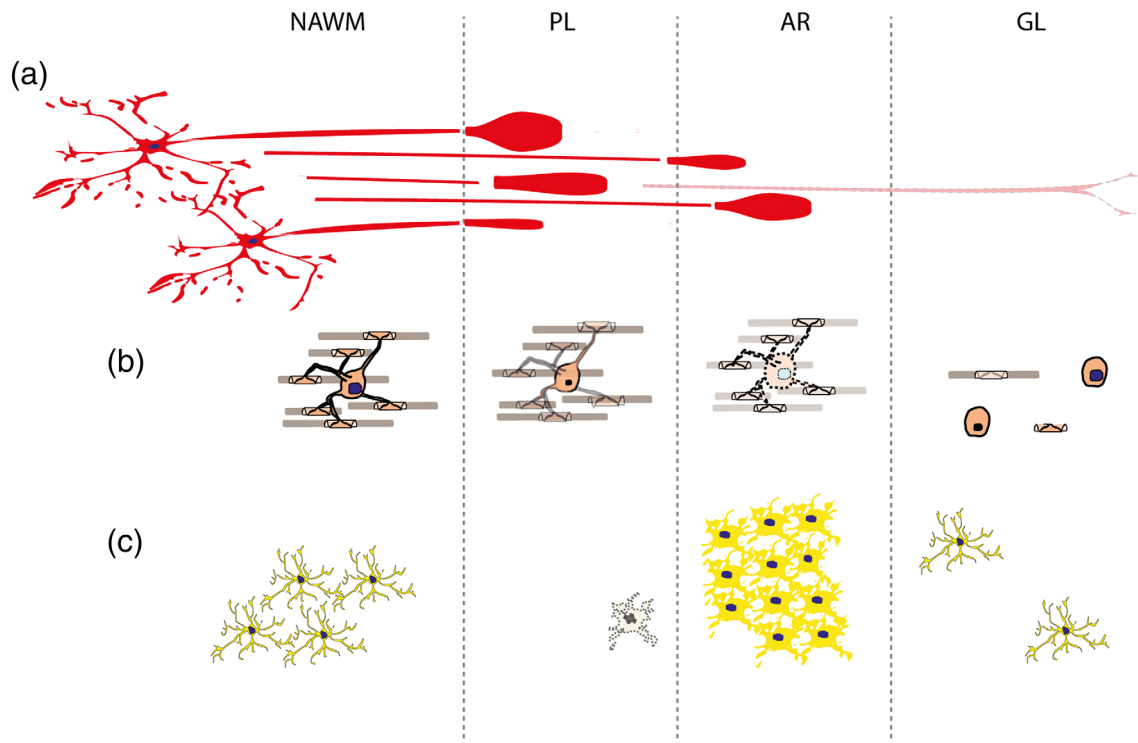


**FIGURE 6** Schematic representation of tissue damage in CALD lesion evolution. (a) Damage to axonal structures starts in prelesional areas (PL) with APP accumulation, spheroid formation and permanent axon loss that further increases in the following actively resorptive (AR) lesion areas, leading to an almost complete absence of axonal structures from gliotic regions (GL). (b) Oligodendrocytes only show minor alterations in PL, whereas major tissue resorption occurs in AR areas. (c) Microglia loss is seen in PL, followed by extensive invasion of foamy phagocytes in AR, and resolution of tissue inflammation in GL areas

past few years it has become increasingly clear that microglia cells play an important role in proper neuronal maturation and functioning (Cserép et al., 2020; Paolicelli et al., 2011; Prinz, Jung, & Priller, 2019). However, there is still limited knowledge on how microglia could specifically support axon maintenance, and axonal damage has not yet been described in animals undergoing transient experimental microglia depletion (Elmore et al., 2014; Rojo et al., 2019). The similarity between PL areas in CALD and ALSP histopathology, specifically the combination of microglia loss and extensive acute axonal damage, as well as the fact that both diseases are responsive to hematopoietic stem cell transplant (Eichler et al., 2017; Gelfand et al., 2020; Mochel et al., 2019), should stimulate further research.

In contrast, the interdependence between oligodendrocytes and axons has been shown in several myelin-mutant models of leukodystrophies where axonal injury emerges secondary to oligodendrocyte impairment. This was attributed to the tight structural and metabolic interactions within the axon-myelin unit (Fünfschilling et al., 2012; Lee et al., 2012; Stadelmann, Timmler, Barrantes-Freer, & Simons, 2019). In his seminal paper on the histopathology of CALD, Schaumburg described prelesional regions preceding areas of massive macrophage infiltration and inflammatory cell cuffing as “demyelination with axonal sparing” (Schaumburg et al., 1975). Accordingly, it was concluded that not only is selective demyelination a central feature in CALD, but in contrast to MS, it occurs even before phagocyte invasion (Ferrer, Aubourg, & Pujol, 2010; Powers, Liu, Moser, &

Moser, 1992). It is important to note, however, that these studies solely relied upon histochemical detection of myelin lipids (LFB) and phagocytes. Our study confirms a reduction in myelin lipid staining intensity in PL areas. However, the gradual, not well demarcated myelin pallor, the concomitant presence of apoptotic oligodendrocytes (Bergner et al., 2019) and the observation of edematous, yet still present myelin by myelin protein immunohistochemistry are generic signs of early myelin damage. In fact, also pre-phagocytic/initial MS lesions are characterized by myelin pallor and edema in LFB histochemistry, indicating subtle myelin injury (Barnett & Prineas, 2004). These early oligodendrocyte and myelin alterations might indeed be an important driver of axonal pathogenic cascades in CALD, as proposed by the above mentioned animal studies. Nevertheless, we provide evidence here that not only in PL areas but, in contrast to MS, also in the foam cell-rich, resorptive lesion stage, myelin is not a selective target of phagocytic removal in CALD. Rather, we observed a comprehensive and concurrent destruction of the entire axon-myelin unit.

Promoting myelin repair is an important therapeutic aim in CALD. However, whether remyelination occurs spontaneously, as is the case in MS (Périer & Grégoire, 1965), and could be exploited therapeutically in CALD is not clear. Impaired differentiation of oligodendrocyte progenitor cells as inferred from epigenomic signatures of normal-appearing CALD white matter was recently proposed to induce a lack of myelin repair in CALD (Schlüter et al., 2018). Examination of myelin lipid and protein phenotypes in CALD did not allow us to identify



brain regions displaying generic features of completed remyelination, that is, shadow plaques as found in MS. To further investigate whether myelin repair pathways are activated in CALD, we used a novel marker protein, BCAS1, specifically delineating newly formed premyelinating and myelinating oligodendrocytes (Fard et al., 2017). We did not observe elevated BCAS1<sup>+</sup> cell densities in the NAWM and PL areas of CALD—in contrast to MS, where BCAS1<sup>+</sup> cells are increased around demyelinated lesions. This may indicate that the subtle myelin pathology seen in PL areas is not sufficient to trigger any remyelination attempts. However, OPC differentiation seems possible in CALD, as we found significantly elevated numbers of branched BCAS1-positive cells in early, less affected AR areas. Importantly, the number of CALD patients with cellular evidence for ongoing myelin regeneration has to be related to the percentage of MS patients with fully remyelinated plaques at autopsy (15–20% Frischer et al., 2015). Furthermore, only a small proportion of shadow plaques in MS display cellular evidence of *ongoing* remyelination as indicated by elevated densities of BCAS1<sup>+</sup> cells (in our cohort 23%).

In summary, our data support a novel view of the sequence of pathogenic events in CALD and thus raise questions with regard to the present histopathologic classification as a primary demyelinating disease. We demonstrate here substantial damage to axons already in PL areas associated with early microglia loss. The phagocytic degradation in actively resorptive (AR) lesion areas does not represent a selective or preferential stripping of myelin sheaths from preserved axons, as is observed in MS. Thus, despite the occurrence of CALD lesion formation in the white matter containing abundant myelin lipids aberrantly enriched with VLCFAs (Powers, Moser, Moser, & Schaumburg, 1982; Powers & Schaumburg, 1981), the disease in our view cannot be classified as primary demyelinating in the strict sense of the term. The unselective resorption of the white matter in CALD is more reminiscent of the removal of comprehensively damaged tissue as occurs, for example, in trauma or ischemia, than of selective myelin targeting as seen in MS. In addition, and further strengthening this point, the present findings indicate that cellular repair pathways *are* activated, and attempts at remyelination *do* prevail in CALD. However, these attempts are immediately beset by ongoing tissue destruction and thus remain largely abortive. Given the subtotal axon loss in advanced gliotic areas, remyelination failure in CALD may not only be due to a relative lack of regenerating oligodendrocytes but also to the absence of an axonal scaffold that could serve as appropriate substrate for remyelination.

There are significant open questions not answered in our study. What is the pathogenic trigger that leads to microglia loss and axonal damage in prelesional areas? How do metabolic alterations and subtle damage of oligodendrocytes contribute? Furthermore, our study does not offer an explanation, why specific regions and tracts of the CNS are particularly vulnerable to become the initial sites of pathology. Nevertheless, we believe, that the re-visited perspective on the sequence of pathogenic events that can be inferred from our observations has important consequences for strategies of therapy development in CALD. It also offers an explanation for the shortcomings of immunomodulatory treatments (Horvath, Eichler, Poskitt, & Stockler-Ipsiroglu, 2012; Rosewich, Nessler, Brück, & Gärtner, 2019).

Furthermore, it would predict that strategies that aim to improve remyelination will be hampered by the absence of functional axons. Thus, our first goal in CALD therapy must be to prohibit axonal destruction right from the onset of disease, and to elucidate the underlying cellular and molecular mechanisms.

## ACKNOWLEDGMENTS

We appreciate the excellent technical support by Katja Schulz, Uta Scheidt, Brigitte Maruschak, Jasmin Reichl, Olga Kowatsch, and Heidi Brodmerkel. We thank Cynthia Bunker for language editing. The present study was supported by the European Leukodystrophies Association (ELA) to Christine Stadelmann, the Deutsche Forschungsgemeinschaft (DFG) transregional collaborative research center (CRC) 274 “Checkpoints of CNS recovery” (Jutta Gärtner, Wolfgang Brück, and Christine Stadelmann), STA 1389/5-1, GA 354/14-1, the DFG under Germany's Excellence Strategy (EXC 2067/1; Jutta Gärtner), the Gemeinnützige Hertie Foundation, the Deutsche Multiple Sklerose Gesellschaft (DMSG, Christine Stadelmann), and the National MS Society (USA, Christine Stadelmann). Caroline G. Bergner was supported as fellow of the Forschungskolleg TRANSMED at the University Medical Center Göttingen by the Ministry of Science and Lower Saxony. Nafiye Genc was supported by the Gemeinnützige Hertie Stiftung as a fellow in the medMS program. Franziska van der Meer held a Dorothea Schlözer postdoctoral stipend of the University Medical Center Göttingen. Jonas Franz is supported by the clinician scientist program of the CRC 274. Open Access funding enabled and organized by Projekt DEAL.

## CONFLICT OF INTEREST

The authors declare no conflict of interest.

## DATA AVAILABILITY STATEMENT

The data that support the findings of this study are available from the corresponding author upon reasonable request.

## ORCID

Caroline G. Bergner  <https://orcid.org/0000-0002-0327-1389>

## REFERENCES

- Barnett, M. H., & Prineas, J. W. (2004). Relapsing and remitting multiple sclerosis: Pathology of the newly forming lesion. *Annals of Neurology*, 55(4), 458–468. <https://doi.org/10.1002/ana.20016>
- de Beer, M., Engelen, M., & van Geel, B. M. (2014). Frequent occurrence of cerebral demyelination in adrenomyeloneuropathy. *Neurology*, 83(24), 2227–2231. <https://doi.org/10.1212/WNL.0000000000001074>
- Berger, J., Forss-Petter, S., & Eichler, F. S. (2014). Pathophysiology of X-linked adrenoleukodystrophy. *Biochimie*, 98, 135–142. <https://doi.org/10.1016/j.biochi.2013.11.023>
- Berger, J., & Gärtner, J. (2006). X-linked adrenoleukodystrophy: Clinical, biochemical and pathogenetic aspects. *Biochimica et Biophysica Acta*, 1763(12), 1721–1732. <https://doi.org/10.1016/j.bbamcr.2006.07.010>
- Bergner, C. G., van der Meer, F., Winkler, A., Wrzos, C., Türkmen, M., Valizada, E., ... Stadelmann, C. (2019). Microglia damage precedes major myelin breakdown in X-linked adrenoleukodystrophy and meta-chromatic leukodystrophy. *Glia*, 67(6), 1196–1209. <https://doi.org/10.1002/glia.23598>

- Bitsch, A., Schuchardt, J., Bunkowski, S., Kuhlmann, T., & Brück, W. (2000). Acute axonal injury in multiple sclerosis. Correlation with demyelination and inflammation. *Brain: A Journal of Neurology*, 123(Pt 6), 1174–1183. <https://doi.org/10.1093/brain/123.6.1174>
- Bjartmar, C., Kidd, G., Mörk, S., Rudick, R., & Trapp, B. D. (2000). Neurological disability correlates with spinal cord axonal loss and reduced N-acetyl aspartate in chronic multiple sclerosis patients. *Annals of Neurology*, 48(6), 893–901.
- Brück, W., Bitsch, A., Kolenda, H., Brück, Y., Stiefel, M., & Lassmann, H. (1997). Inflammatory central nervous system demyelination: Correlation of magnetic resonance imaging findings with lesion pathology. *Annals of Neurology*, 42(5), 783–793. <https://doi.org/10.1002/ana.410420515>
- Charcot, J. M. (1868). *Histologie de la sclerose en plaques, leçon faite à l'hospice de la salpêtrière*. HACHETTE LIVRE: BNF.
- Coleman, M. (2005). Axon degeneration mechanisms: Commonality amid diversity. *Nature Reviews Neuroscience*, 6(11), 889–898. <https://doi.org/10.1038/nrn1788>
- Cserép, C., Pósfai, B., Lénárt, N., Fekete, R., László, Z. I., Lele, Z., Orsolits, B., Molnár, G., Heindl, S., Schwarcz, A. D., Ujvári, K., Környei, Z., Tóth, K., Szabadits, E., Sperlágh, B., Baranyi, M., Csiba, L., Hortobágyi, T., Maglóczky, Z., ... Dénes, Á. (2020). Microglia monitor and protect neuronal function through specialized somatic purinergic junctions. *Science (New York, N.Y.)*, 367(6477), 528–537. <https://doi.org/10.1126/science.aax6752>
- Eichler, F. S., Barker, P. B., Cox, C., Edwin, D., Ulug, A. M., Moser, H. W., & Raymond, G. V. (2002). Proton MR spectroscopic imaging predicts lesion progression on MRI in X-linked adrenoleukodystrophy. *Neurology*, 58(6), 901–907. <https://doi.org/10.1212/wnl.58.6.901>
- Eichler, F., Duncan, C., Musolino, P. L., Orchard, P. J., de Oliveira, S., Thrasher, A. J., Armant, M., Dansereau, C., Lund, T. C., Miller, W. P., Raymond, G. V., Sankar, R., Shah, A. J., Sevin, C., Gaspar, H. B., Gissen, P., Amartino, H., Bratkovic, D., Smith, N. J. C., ... Williams, D. A. (2017). Hematopoietic stem-cell gene therapy for cerebral adrenoleukodystrophy. *The New England Journal of Medicine*, 377(17), 1630–1638. <https://doi.org/10.1056/NEJMoa1700554>
- Eichler, F. S., Itoh, R., Barker, P. B., Mori, S., Garrett, E. S., van Zijl, P. C. M., Moser, H. W., Raymond, G. V., & Melhem, E. R. (2002). Proton MR spectroscopic and diffusion tensor brain MR imaging in X-linked adrenoleukodystrophy: Initial experience. *Radiology*, 225(1), 245–252. <https://doi.org/10.1148/radiol.2251011040>
- Eichler, F. S., Ren, J.-Q., Cossoy, M., Rietsch, A. M., Nagpal, S., Moser, A. B., Frosch, M. P., & Ransohoff, R. M. (2008). Is microglial apoptosis an early pathogenic change in cerebral X-linked adrenoleukodystrophy? *Annals of Neurology*, 63(6), 729–742. <https://doi.org/10.1002/ana.21391>
- Elmore, M. R. P., Najafi, A. R., Koike, M. A., Dagher, N. N., Spangenberg, E. E., Rice, R. A., Kitazawa, M., Matusow, B., Nguyen, H., West, B. L., & Green, K. N. (2014). Colony-stimulating factor 1 receptor signaling is necessary for microglia viability, unmasking a microglia progenitor cell in the adult brain. *Neuron*, 82(2), 380–397. <https://doi.org/10.1016/j.neuron.2014.02.040>
- Engelen, M., Kemp, S., & Poll-The, B.-T. (2014). X-linked adrenoleukodystrophy: Pathogenesis and treatment. *Current Neurology and Neuroscience Reports*, 14(10), 486. <https://doi.org/10.1007/s11910-014-0486-0>
- Fard, M. K., van der Meer, F., Sánchez, P., Cantuti-Castelvetri, L., Mandad, S., Jäkel, S., Fornasiero, E. F., Schmitt, S., Ehrlich, M., Starost, L., Kuhlmann, T., Sergiou, C., Schultz, V., Wrzos, C., Brück, W., Urlaub, H., Dimou, L., Stadelmann, C., & Simons, M. (2017). Bcas1 expression defines a population of early myelinating oligodendrocytes in multiple sclerosis lesions. *Science Translational Medicine*, 9(419), eaam7816. <https://doi.org/10.1126/scitranslmed.aam7816>
- Ferguson, B., Matyszak, M. K., Esiri, M. M., & Perry, V. H. (1997). Axonal damage in acute multiple sclerosis lesions. *Brain: A Journal of Neurology*, 120(Pt 3), 393–399. <https://doi.org/10.1093/brain/120.3.393>
- Ferrer, I., Aubourg, P., & Pujol, A. (2010). General aspects and neuropathology of X-linked adrenoleukodystrophy. *Brain Pathology (Zurich, Switzerland)*, 20(4), 817–830. <https://doi.org/10.1111/j.1750-3639.2010.00390.x>
- Fouquet, F., Zhou, J. M., Ralston, E., Murray, K., Troalen, F., Magal, E., Robain, O., Dubois-Dalcq, M., & Aubourg, P. (1997). Expression of the adrenoleukodystrophy protein in the human and mouse central nervous system. *Neurobiology of Disease*, 3(4), 271–285. <https://doi.org/10.1006/nbdi.1997.0127>
- Fourcade, S., Ferrer, I., & Pujol, A. (2015). Oxidative stress, mitochondrial and proteostasis malfunction in adrenoleukodystrophy: A paradigm for axonal degeneration. *Free Radical Biology & Medicine*, 88, 18–29. <https://doi.org/10.1016/j.freeradbiomed.2015.05.041>
- Frischer, J. M., Bramow, S., Dal-Bianco, A., Lucchinetti, C. F., Rauschka, H., Schmidbauer, M., Laursen, H., Sorensen, P. S., & Lassmann, H. (2009). The relation between inflammation and neurodegeneration in multiple sclerosis brains. *Brain: A Journal of Neurology*, 132(5), 1175–1189. <https://doi.org/10.1093/brain/awp070>
- Frischer, J. M., Weigand, S. D., Guo, Y., Kale, N., Parisi, J. E., Pirko, I., Mandrekar, J., Bramow, S., Metz, I., Brück, W., Lassmann, H., & Lucchinetti, C. F. (2015). Clinical and pathological insights into the dynamic nature of the white matter multiple sclerosis plaque. *Annals of Neurology*, 78(5), 710–721. <https://doi.org/10.1002/ana.24497>
- Fünfschilling, U., Supplie, L. M., Mahad, D., Boretius, S., Saab, A. S., Edgar, J., Brinkmann, B. G., Kassmann, C. M., Tzvetanova, I. D., Möbius, W., Diaz, F., Meijer, D., Suter, U., Hamprecht, B., Sereda, M. W., Moraes, C. T., Frahm, J., Goebbels, S., & Nave, K.-A. (2012). Glycolytic oligodendrocytes maintain myelin and long-term axonal integrity. *Nature*, 485(7399), 517–521. <https://doi.org/10.1038/nature11007>
- Gelfand, J. M., Greenfield, A. L., Barkovich, M., Mendelsohn, B. A., van Haren, K., Hess, C. P., & Mannis, G. N. (2020). Allogeneic HSCT for adult-onset leukoencephalopathy with spheroids and pigmented glia. *Brain: A Journal of Neurology*, 143(2), 503–511. <https://doi.org/10.1093/brain/awz390>
- Gong, Y., Sasidharan, N., Laheji, F., Frosch, M., Musolino, P., Tanzi, R., Kim, D. Y., Biffi, A., el Khoury, J., & Eichler, F. (2017). Microglial dysfunction as a key pathological change in adrenomyeloneuropathy. *Annals of Neurology*, 82(5), 813–827. <https://doi.org/10.1002/ana.25085>
- Görtz, A. L., Peferoen, L. A. N., Gerritsen, W. H., van Noort, J. M., Bugiani, M., & Amor, S. (2018). Heat shock protein expression in cerebral X-linked adrenoleukodystrophy reveals astrocyte stress prior to myelin loss. *Neuropathology and Applied Neurobiology*, 44(4), 363–376. <https://doi.org/10.1111/nan.12399>
- Höftberger, R., Kunze, M., Weinhofer, I., Aboul-Enein, F., Voigtländer, T., Oezen, I., ... Berger, J. (2007). Distribution and cellular localization of adrenoleukodystrophy protein in human tissues: Implications for X-linked adrenoleukodystrophy. *Neurobiology of Disease*, 28(2), 165–174. <https://doi.org/10.1016/j.nbd.2007.07.007>
- Horvath, G. A., Eichler, F., Poskitt, K., & Stockler-Ipsiroglu, S. (2012). Failure of repeated cyclophosphamide pulse therapy in childhood cerebral X-linked adrenoleukodystrophy. *Neuropediatrics*, 43(1), 48–52. <https://doi.org/10.1055/s-0032-1307455>
- Kemp, S., Pujol, A., Waterham, H. R., van Geel, B. M., Boehm, C. D., Raymond, G. V., ... Moser, H. W. (2001). Abcd1 mutations and the X-linked adrenoleukodystrophy mutation database: Role in diagnosis and clinical correlations. *Human Mutation*, 18(6), 499–515. <https://doi.org/10.1002/humu.1227>
- Konno, T., Kasanuki, K., Ikeuchi, T., Dickson, D. W., & Wszolek, Z. K. (2018). Csf1r-related leukoencephalopathy: A major player in primary microgliopathies. *Neurology*, 91(24), 1092–1104. <https://doi.org/10.1212/WNL.0000000000006642>
- Koo, E. H., Sisodia, S. S., Archer, D. R., Martin, L. J., Weidemann, A., Beyreuther, K., Fischer, P., Masters, C. L., & Price, D. L. (1990). Precursor of amyloid protein in Alzheimer disease undergoes fast



- anterograde axonal transport. *Proceedings of the National Academy of Sciences of the United States of America*, 87(4), 1561–1565. <https://doi.org/10.1073/pnas.87.4.1561>
- Kuhlmann, T., Lingfeld, G., Bitsch, A., Schuchardt, J., & Brück, W. (2002). Acute axonal damage in multiple sclerosis is most extensive in early disease stages and decreases over time. *Brain: A Journal of Neurology*, 125(Pt 10), 2202–2212. <https://doi.org/10.1093/brain/awf235>
- Kuhlmann, T., Ludwin, S., Prat, A., Antel, J., Brück, W., & Lassmann, H. (2017). An updated histological classification system for multiple sclerosis lesions. *Acta Neuropathologica*, 133(1), 13–24. <https://doi.org/10.1007/s00401-016-1653-y>
- Lee, Y., Morrison, B. M., Li, Y., Lengacher, S., Farah, M. H., Hoffman, P. N., Liu, Y., Tsingalia, A., Jin, L., Zhang, P. W., Pellerin, L., Magistretti, P. J., & Rothstein, J. D. (2012). Oligodendroglia metabolically support axons and contribute to neurodegeneration. *Nature*, 487(7408), 443–448. <https://doi.org/10.1038/nature11314>
- Liberato, A. P., Mallack, E. J., Aziz-Bose, R., Hayden, D., Lauer, A., Caruso, P. A., Musolino, P. L., & Eichler, F. S. (2019). Mri brain lesions in asymptomatic boys with X-linked adrenoleukodystrophy. *Neurology*, 92(15), e1698–e1708. <https://doi.org/10.1212/WNL.00000000000007294>
- Mahad, D. H., Trapp, B. D., & Lassmann, H. (2015). Pathological mechanisms in progressive multiple sclerosis. *The Lancet Neurology*, 14(2), 183–193. [https://doi.org/10.1016/S1474-4422\(14\)70256-X](https://doi.org/10.1016/S1474-4422(14)70256-X)
- Mahmood, A., Raymond, G. V., Dubey, P., Peters, C., & Moser, H. W. (2007). Survival analysis of haematopoietic cell transplantation for childhood cerebral X-linked adrenoleukodystrophy: A comparison study. *The Lancet Neurology*, 6(8), 687–692. [https://doi.org/10.1016/S1474-4422\(07\)70177-1](https://doi.org/10.1016/S1474-4422(07)70177-1)
- Mallack, E. J., van de Stadt, S., Caruso, P. A., Musolino, P. L., Sadjadi, R., Engelen, M., & Eichler, F. S. (2020). Clinical and radiographic course of arrested cerebral adrenoleukodystrophy. *Neurology*, 94(24), e2499–e2507. <https://doi.org/10.1212/WNL.00000000000009626>
- Mochel, F., Delorme, C., Czernecki, V., Froger, J., Cormier, F., Ellie, E., Fegueux, N., Lehéry, S., Lumbroso, S., Schiffmann, R., Aubourg, P., Roze, E., Labauge, P., & Nguyen, S. (2019). Haematopoietic stem cell transplantation in CSF1R-related adult-onset leukoencephalopathy with axonal spheroids and pigmented glia. *Journal of Neurology, Neurosurgery, and Psychiatry*, 90(12), 1375–1376. <https://doi.org/10.1136/jnnp-2019-320701>
- Moser, H. W., Naidu, S., Kumar, A. J., & Rosenbaum, A. E. (1987). The adrenoleukodystrophies. *Critical Reviews in Neurobiology*, 3(1), 29–88.
- Mosser, J., Douar, A. M., Sarde, C. O., Kioschis, P., Feil, R., Moser, H., Poustka, A. M., Mandel, J. L., & Aubourg, P. (1993). Putative X-linked adrenoleukodystrophy gene shares unexpected homology with ABC transporters. *Nature*, 361(6414), 726–730. <https://doi.org/10.1038/361726a0>
- Musolino, P. L., Gong, Y., Snyder, J. M. T., Jimenez, S., Lok, J., Lo, E. H., Moser, A. B., Grabowski, E. F., Frosch, M. P., & Eichler, F. S. (2015). Brain endothelial dysfunction in cerebral adrenoleukodystrophy. *Brain: A Journal of Neurology*, 138(Pt 11), 3206–3220. <https://doi.org/10.1093/brain/awv250>
- Oosterhof, N., Chang, I. J., Karimiani, E. G., Kuil, L. E., Jensen, D. M., Daza, R., Young, E., Astle, L., van der Linde, H. C., Shivaram, G. M., Demmers, J., Latimer, C. S., Keene, C. D., Loter, E., Maroofian, R., van Ham, T. J., Hevner, R. F., & Bennett, J. T. (2019). Homozygous mutations in CSF1R cause a pediatric-onset leukoencephalopathy and can result in congenital absence of microglia. *American Journal of Human Genetics*, 104(5), 936–947. <https://doi.org/10.1016/j.ajhg.2019.03.010>
- Oyanagi, K., Kinoshita, M., Suzuki-Kouyama, E., Inoue, T., Nakahara, A., Tokiwai, M., ... Ikeda, S.-I. (2017). Adult onset leukoencephalopathy with axonal spheroids and pigmented glia (ALSP) and Nasu-Hakola disease: Lesion staging and dynamic changes of axons and microglial subsets. *Brain Pathology (Zurich, Switzerland)*, 27(6), 748–769. <https://doi.org/10.1111/bpa.12443>
- Paolicelli, R. C., Bolasco, G., Pagani, F., Maggi, L., Scianni, M., Panzanelli, P., Giustetto, M., Ferreira, T. A., Guiducci, E., Dumas, L., Ragozzino, D., & Gross, C. T. (2011). Synaptic pruning by microglia is necessary for normal brain development. *Science (New York, N.Y.)*, 333(6048), 1456–1458. <https://doi.org/10.1126/science.1202529>
- Patrikios, P., Stadelmann, C., Kutzelnigg, A., Rauschka, H., Schmidbauer, M., Laursen, H., Sorensen, P. S., Bruck, W., Lucchinetti, C., & Lassmann, H. (2006). Remyelination is extensive in a subset of multiple sclerosis patients. *Brain: A Journal of Neurology*, 129(Pt 12), 3165–3172. <https://doi.org/10.1093/brain/awl217>
- Périer, O., & Grégoire, A. (1965). Electron microscopic features of multiple sclerosis lesions. *Brain: A Journal of Neurology*, 88(5), 937–952. <https://doi.org/10.1093/brain/88.5.937>
- Powers, J. M., Liu, Y., Moser, A. B., & Moser, H. W. (1992). The inflammatory myelinopathy of adreno-leukodystrophy: Cells, effector molecules, and pathogenetic implications. *Journal of Neuropathology and Experimental Neurology*, 51(6), 630–643. <https://doi.org/10.1097/00005072-199211000-00007>
- Powers, J. M., & Schaumburg, H. H. (1981). The testis in adreno-leukodystrophy. *The American Journal of Pathology*, 102(1), 90–98.
- Powers, J. M., Moser, H. W., Moser, A. B., & Schaumburg, H. H. (1982). Fetal adrenoleukodystrophy: The significance of pathologic lesions in adrenal gland and testis. *Human Pathology*, 13(11), 1013–1019. [https://doi.org/10.1016/S0046-8177\(82\)80093-2](https://doi.org/10.1016/S0046-8177(82)80093-2)
- Prinz, M., Jung, S., & Priller, J. (2019). Microglia biology: One century of evolving concepts. *Cell*, 179(2), 292–311. <https://doi.org/10.1016/j.cell.2019.08.053>
- Pujol, A., Ferrer, I., Camps, C., Metzger, E., Hindelang, C., Callizot, N., Ruiz, M., Pàmpol, T., Giròs, M., & Mandel, J. L. (2004). Functional overlap between ABCD1 (ALD) and ABCD2 (ALDR) transporters: A therapeutic target for X-adrenoleukodystrophy. *Human Molecular Genetics*, 13(23), 2997–3006. <https://doi.org/10.1093/hmg/ddh323>
- Pujol, A., Hindelang, C., Callizot, N., Bartsch, U., Schachner, M., & Mandel, J. L. (2002). Late onset neurological phenotype of the X-ALD gene inactivation in mice: A mouse model for adrenomyeloneuropathy. *Human Molecular Genetics*, 11(5), 499–505. <https://doi.org/10.1093/hmg/11.5.499>
- Radzun, H. J., Hansmann, M. L., Heidebrecht, H. J., Bödewadt-Radzun, S., Wacker, H. H., Kreipe, H., Lumbeck, H., Hernandez, C., Kuhn, C., & Parwaresch, M. R. (1991). Detection of a monocyte/macrophage differentiation antigen in routinely processed paraffin-embedded tissues by monoclonal antibody Ki-M1P. *Laboratory Investigation: A Journal of Technical Methods and Pathology*, 65(3), 306–315.
- Raymond, G. V., Aubourg, P., Paker, A., Escolar, M., Fischer, A., Blanche, S., Baruchel, A., Dalle, J. H., Michel, G., Prasad, V., Miller, W., Paadre, S., Balsler, J., Kurtzberg, J., Nascene, D. R., Orchard, P. J., & Lund, T. (2019). Survival and functional outcomes in boys with cerebral adrenoleukodystrophy with and without hematopoietic stem cell transplantation. *Biology of Blood and Marrow Transplantation: Journal of the American Society for Blood and Marrow Transplantation*, 25(3), 538–548. <https://doi.org/10.1016/j.bbmt.2018.09.036>
- Rojo, R., Raper, A., Ozdemir, D. D., Lefevre, L., Grabert, K., Wollscheid-Lengeling, E., Bradford, B., Caruso, M., Gazova, I., Sánchez, A., Lisowski, Z. M., Alves, J., Molina-Gonzalez, I., Davtyan, H., Lodge, R. J., Glover, J. D., Wallace, R., Munro, D. A. D., David, E., ... Pridans, C. (2019). Deletion of a Csf1r enhancer selectively impacts CSF1R expression and development of tissue macrophage populations. *Nature Communications*, 10(1), 3215. <https://doi.org/10.1038/s41467-019-11053-8>
- Rosewich, H., Nessler, S., Brück, W., & Gärtner, J. (2019). B cell depletion can be effective in multiple sclerosis but failed in a patient with advanced childhood cerebral X-linked adrenoleukodystrophy.

- Therapeutic Advances in Neurological Disorders*, 12. <https://doi.org/10.1177/1756286419868133>
- Schaumburg, H. H., Powers, J. M., Raine, C. S., Suzuki, K., & Richardson, E. P. (1975). Adrenoleukodystrophy. A clinical and pathological study of 17 cases. *Archives of Neurology*, 32(9), 577–591. <https://doi.org/10.1001/archneur.1975.00490510033001>
- Schlüter, A., Sandoval, J., Fourcade, S., Díaz-Lagares, A., Ruiz, M., Casaccia, P., Esteller, M., & Pujol, A. (2018). Epigenomic signature of adrenoleukodystrophy predicts compromised oligodendrocyte differentiation. *Brain Pathology (Zurich, Switzerland)*, 28(6), 902–919. <https://doi.org/10.1111/bpa.12595>
- Siffrin, V., Radbruch, H., Glumm, R., Niesner, R., Paterka, M., Herz, J., Leuenberger, T., Lehmann, S. M., Luenstedt, S., Rinnenthal, J. L., Laube, G., Luche, H., Lehnardt, S., Fehling, H. J., Griesbeck, O., & Zipp, F. (2010). In vivo imaging of partially reversible th17 cell-induced neuronal dysfunction in the course of encephalomyelitis. *Immunity*, 33(3), 424–436. <https://doi.org/10.1016/j.immuni.2010.08.018>
- Spencer, P. S., & Schaumburg, H. H. (1977a). Ultrastructural studies of the dying-back process. III. The evolution of experimental peripheral giant axonal degeneration. *Journal of Neuropathology and Experimental Neurology*, 36(2), 276–299. <https://doi.org/10.1097/00005072-197703000-00005>
- Spencer, P. S., & Schaumburg, H. H. (1977b). Ultrastructural studies of the dying-back process. IV. Differential vulnerability of PNS and CNS fibers in experimental central-peripheral distal axonopathies. *Journal of Neuropathology and Experimental Neurology*, 36(2), 300–320. <https://doi.org/10.1097/00005072-197703000-00006>
- Stadelmann, C., Timmler, S., Barrantes-Freer, A., & Simons, M. (2019). Myelin in the central nervous system: Structure, function, and pathology. *Physiological Reviews*, 99(3), 1381–1431. <https://doi.org/10.1152/physrev.00031.2018>
- Stys, P. K. (2005). General mechanisms of axonal damage and its prevention. *Journal of the Neurological Sciences*, 233(1–2), 3–13. <https://doi.org/10.1016/j.jns.2005.03.031>
- Theda, C., Moser, A. B., Powers, J. M., & Moser, H. W. (1992). Phospholipids in X-linked adrenoleukodystrophy white matter: Fatty acid abnormalities before the onset of demyelination. *Journal of the Neurological Sciences*, 110(1–2), 195–204. [https://doi.org/10.1016/0022-510X\(92\)90028-J](https://doi.org/10.1016/0022-510X(92)90028-J)
- Trapp, B. D., Peterson, J., Ransohoff, R. M., Rudick, R., Mörk, S., & Bö, L. (1998). Axonal transection in the lesions of multiple sclerosis. *The New England Journal of Medicine*, 338(5), 278–285. <https://doi.org/10.1056/NEJM199801293380502>
- Trapp, B. D., Vignos, M., Dudman, J., Chang, A., Fisher, E., Staugaitis, S. M., Battapady, H., Mork, S., Ontaneda, D., Jones, S. E., Fox, R. J., Chen, J., Nakamura, K., & Rudick, R. A. (2018). Cortical neuronal densities and cerebral white matter demyelination in multiple sclerosis: A retrospective study. *The Lancet Neurology*, 17(10), 870–884. [https://doi.org/10.1016/S1474-4422\(18\)30245-X](https://doi.org/10.1016/S1474-4422(18)30245-X)
- Weber, F. D., Wiesinger, C., Forss-Petter, S., Regelsberger, G., Einwich, A., Weber, W. H. A., Kohler, W., Stockinger, H., & Berger, J. (2014). X-linked adrenoleukodystrophy: Very long-chain fatty acid metabolism is severely impaired in monocytes but not in lymphocytes. *Human Molecular Genetics*, 23(10), 2542–2550. <https://doi.org/10.1093/hmg/ddt645>
- Weinhofer, I., Zierfuss, B., Hametner, S., Wagner, M., Popitsch, N., Machacek, C., ... Berger, J. (2018). Impaired plasticity of macrophages in X-linked adrenoleukodystrophy. *Brain: A Journal of Neurology*, 141(8), 2329–2342. <https://doi.org/10.1093/brain/awy127>
- Yang, J., Weimer, R. M., Kallop, D., Olsen, O., Wu, Z., Renier, N., Uryu, K., & Tessier-Lavigne, M. (2013). Regulation of axon degeneration after injury and in development by the endogenous calpain inhibitor calpastatin. *Neuron*, 80(5), 1175–1189. <https://doi.org/10.1016/j.neuron.2013.08.034>

#### SUPPORTING INFORMATION

Additional supporting information may be found online in the Supporting Information section at the end of this article.

**How to cite this article:** Bergner, C. G., Genc, N., Hametner, S., Franz, J., van der Meer, F., Mitkovski, M., Weber, M. S., Stoltenburg-Didinger, G., Kühl, J.-S., Köhler, W., Brück, W., Gärtner, J., & Stadelmann, C. (2021). Concurrent axon and myelin destruction differentiates X-linked adrenoleukodystrophy from multiple sclerosis. *Glia*, 69(10), 2362–2377. <https://doi.org/10.1002/glia.24042>